

# Correction and analysis of lead content in soil by laser-induced breakdown spectroscopy

Chengli Xie (谢承利)<sup>1\*</sup>, Jidong Lu (陆继东)<sup>1\*\*</sup>, Pengyan Li (李鹏艳)<sup>1</sup>,  
Jie Li (李捷)<sup>1</sup>, and Zhaoxiang Lin (林光祥)<sup>2</sup>

<sup>1</sup>State Key Laboratory of Coal Combustion, Huazhong University of Science and Technology, Wuhan 430074, China

<sup>2</sup>College of Electrics and Information Engineering, South-Central University for Nationalities, Wuhan 430074, China

\*E-mail: chenry\_xie@sina.com.cn; \*\*e-mail: jdllu@mail.hust.edu.cn

Received October 7, 2008

The laser-induced breakdown spectroscopy is used to analyze the lead content in soils. The analyzed spectral line profile is fitted by Lorentzian function for determining the background and the full-width at half-maximum (FWHM) intensity of spectral line. A self-absorption correction model based on the information of spectral broadening is introduced to calculate the true value of spectral line intensity, which refers to the elemental concentration. The results show that the background intensity obtained by spectral profile fitting is very effective and important due to removing the interference of spectral broadening, and a better precision of calibration analysis is acquired by correcting the self-absorption effect.

OCIS codes: 300.0300, 330.1880.

doi: 10.3788/COL20090706.0545.

Laser-induced breakdown spectroscopy (LIBS) has been researched as a diagnostic tool of composition analysis since the early 1980s, and has developed rapidly for many purposes over the past two decades, such as identifying elements, material identification, process monitoring, material sorting, and site screening<sup>[1]</sup>. The LIBS technique offers the prospect of non-destructive, *in situ*, rapid, and highly selective and sensitive detection and analysis of both natural and man-made materials. Especially, LIBS combining with fiber optic technology brings the potential for designing a portable and standoff distance LIBS analyzer, which is required highly in environmental pollution monitoring.

The early research institutes in the environmental application of LIBS included Diagnostics Instrumentation and Analysis Laboratory (DIAL) at Mississippi State University and US Army Research Laboratory (ARL), which respectively analyzed the contaminated soil from army site and detected the resources conservation and toxic heavy metals in the off-gas of industrial plants and in liquids<sup>[2,3]</sup>. The application of LIBS on the analysis of polluted soils, especially on the detection of noxious heavy metals, was investigated by some other researchers<sup>[4]</sup>. Recently, LIBS was researched on the detection of lunar soil for moon exploration<sup>[5]</sup>. Much work was addressed to the important issues of sensitivity and analytic precision, and the quantitative analysis was verified universally to be influenced remarkably by the variation of matrix component and self-absorption phenomenon in optical emission spectroscopy<sup>[6,7]</sup>. The well-known curve of growth (COG) method was used by Bulajic *et al.*<sup>[8]</sup> for correcting the self-absorption effect in calibration-free LIBS. A self-absorption model in LIBS measurements on soils and sediments was constructed for correcting the calibration curves of intensity by Lazic *et al.*<sup>[9]</sup>. These models are generally based on detailed plasma parameters such as size, temperature, electron density, and so on, some of which are hard to be obtained or involve complicated calculation. In this letter,

the contaminated soil with wide range concentration of lead element is analyzed by LIBS. The spectral profile of Pb 405.78-nm atomic emission line is fitted in Lorentzian curve according to the main broadening mechanism of LIBS. Also a correction model is introduced to calculate the influence degree of self-absorption on the net line intensity, and the effectiveness of the model is verified experimentally.

The degree of spectral line self-absorption is parameterized by the self-absorption coefficient (SAC), which is defined as the ratio of the measured spectral line peak intensity to the spectral line peak intensity without self-absorption. With this definition, SAC is equal to 1 if the line is not self-absorbed and decreases towards 0 if the self-absorption increases. According to the classic spectroscopy theory<sup>[10,11]</sup>, the emission spectral line peak intensity ( $W/cm^3$ ) corresponding to the transition from the upper level  $j$  to the lower level  $i$  of an excited atom or ion is determined by

$$I(\lambda) = F \frac{8\pi hc^2 n_j g_j}{\lambda_0^3 n_i g_i} (1 - e^{-k(\lambda)l}). \quad (1)$$

If the plasma is assumed optically thin, i.e., the self-absorption is absent and  $k(\lambda)l \ll 1$ , the spectral line peak intensity  $I_0(\lambda)$  can be approximated as

$$I_0(\lambda) \approx F \frac{8\pi hc^2 n_j g_j}{\lambda_0^3 n_i g_i} k(\lambda)l. \quad (2)$$

In Eqs. (1) and (2),  $F$  is a constant factor depending on the measuring instrument,  $h$  is the Planck constant (J·s),  $c$  is the speed of light (m/s),  $\lambda_0$  is the transition wavelength (m),  $n_j$ ,  $n_i$ ,  $g_j$ , and  $g_i$  are the number densities ( $cm^{-3}$ ) and the degeneracies (dimensionless) of the upper and the ground atomic levels (for the resonance transition), respectively,  $k(\lambda)$  is the frequency-dependent absorption coefficient ( $cm^{-1}$ ), and  $l$  is the absorption path length (cm).

The absorption coefficient  $k(\lambda)$  follows a Voigt distribution, the convolution of a Gaussian function, and a Lorentzian function. But in the typical LIBS conditions, the Lorentzian contribution led by collision broadening and natural line broadening is dominant absolutely. Thus  $k(\lambda)l$  can be expressed as

$$k(\lambda)l \approx K \frac{\Delta\lambda_0}{4(\lambda - \lambda_0)^2 + \Delta\lambda_0^2}, \quad (3)$$

where  $K = 2e^2n_i f \lambda_0^2 l / mc^2$ ,  $e$  and  $m$  are the charge and the mass (g) of the electron,  $f$  is the oscillator strength (dimensionless) of the transition, and  $\Delta\lambda_0$  is the line full-width at half-maximum (FWHM) intensity without self-absorption.

According to the definition of SAC and the above equations, the SAC of spectral line  $\lambda_0$  can be expressed as

$$\text{SAC} = \frac{I(\lambda_0)}{I_0(\lambda_0)} = \frac{\Delta\lambda_0(1 - e^{-\frac{K}{\Delta\lambda_0}})}{K}. \quad (4)$$

In addition, the definition of FWHM has an inclusion relation that for  $\lambda = \lambda_0 \pm \lambda/2$  the intensity  $I(\lambda)$  must be equal to  $I(\lambda_0)/2$ . Combining Eqs. (1) and (3), the relation between the real linewidth  $\Delta\lambda$  and the ideal linewidth  $\Delta\lambda_0$  can be deduced as

$$\frac{(1 - e^{-\frac{K}{\Delta\lambda^2 + \Delta\lambda_0^2}})}{1 - e^{-\frac{K}{\Delta\lambda_0^2}}} = \frac{1}{2}. \quad (5)$$

By numerically solving Eqs. (4) and (5), a relational expression of  $\Delta\lambda$ ,  $\Delta\lambda_0$ , and SAC exists as

$$\frac{\Delta\lambda}{\Delta\lambda_0} = (\text{SAC})^{-0.54}. \quad (6)$$

In Eq. (6),  $\Delta\lambda$  can be gained from the real measured spectral data, and  $\Delta\lambda_0$  is equal to the Stark broadening of analytic line. For typical LIBS conditions, the contribution from ion broadening is negligible, and the Stark broadening of a line is given by<sup>[2]</sup>

$$\Delta\lambda_0 = \Delta\lambda_{\text{Stark}} = 2w(n_e \times 10^{-16}), \quad (7)$$

where  $w$  is the electron impact parameter of analytic line, and  $n_e$  is the electron density that can be counted by the information of other emission line that belongs to the very low density atom or ion, which means weak and negligible self-absorption.

The LIBS system used for obtaining the spectra analyzed in this letter is schematically presented in Fig. 1. The experimental apparatus uses a Q-switched Nd:YAG laser (Pro290, Spectra-Physics Company), delivering about 600 mJ at 1064 nm in 10-ns pulses, at a maximum repetition rate of 10 Hz, for generating a micro-plasma at the sample surface. The laser beam passes through an optical attenuator to reduce the pulse energy to 180 mJ and is focused on the surface of samples by a lens of 32-cm focal length. The light emitted from the excited plasma plume is collected by an optical system and then sent through an optical fiber to an imaging system, which includes an echelle spectrometer (ME5000, Andor Technology) coupled with an intensified charge coupled device (ICCD) camera (iStar DH734, Andor Technology).

The working wavelength range of the imaging system is 200–850 nm with a spectral resolution of  $\lambda/\Delta\lambda=5000$  (corresponding to 3 pixels FWHM). The laser source and imaging system are controlled by a Stanford DG535 pulse/delay generator. A signal synchronized to the laser Q-switch is used for the triggering of the generator to minimize the timing jitter. The delay trigger implements adjustment of the time difference between the laser pulse shot and ICCD time gating. The samples are fixed on a rotatable stage to ensure a fresh surface available for each laser shot. The collection apparatus (quartz optical fiber) is placed close to the plume under an angle of 45° with the sample surface to collect the plasma emission.

The samples used in this work were precisely prepared. The natural soil was taken from field ground and dried in the air, and then was milled into the powder. The dry soil powder was mixed with different weights of lead chloride reagents to form some homogeneous samples containing different lead contents. All the samples were pressed to pellets. The distributions of Pb concentrations in samples is shown in Table 1.

In the previous work<sup>[12]</sup>, it has been demonstrated that the proper delay time of ICCD gating after the plasma generating is effective for the reduction of continuum bremsstrahlung emission background as well as for the improvement of the signal-to-noise ratio (SNR). Figure 2 shows the evolution of the intensity and SNR of Pb 405.78-nm spectral line in the No. 3 sample during the delay time changing, and the gate width is set to 1.0 μs. It is clear that the line intensity decreases and the SNR increases when the delay time increases. Considering the integrated optimization of the line intensity and SNR, a delay time of 0.7 μs was chosen for all the experimental investigation in this work, and accordingly the gate width was 1.0 μs.

In the LIBS measurement, the spectral line intensity should be the net line intensity by subtracting the background. Thus, confirming the exact spectral background is a very important process that impacts on the accuracy of LIBS analysis. Usually, the mean of the both bottom sides of the analyzed line peak is regarded as the value of background. However, the background value

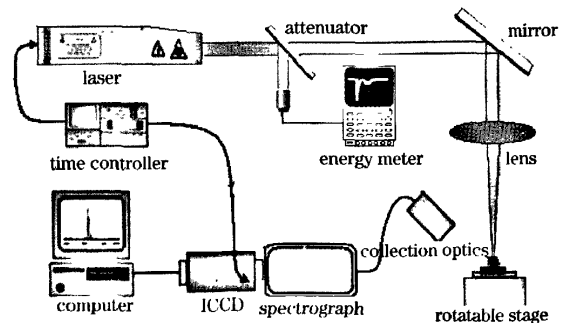


Fig. 1. Schematic diagram of the experimental setup.

Table 1. Pb Concentrations in Samples

| No.       | 1 | 2  | 3  | 4  | 5   | 6   | 7   | 8    | 9    | 10   |
|-----------|---|----|----|----|-----|-----|-----|------|------|------|
| Pb (μg/g) | 4 | 19 | 37 | 60 | 134 | 238 | 931 | 1862 | 3723 | 7446 |

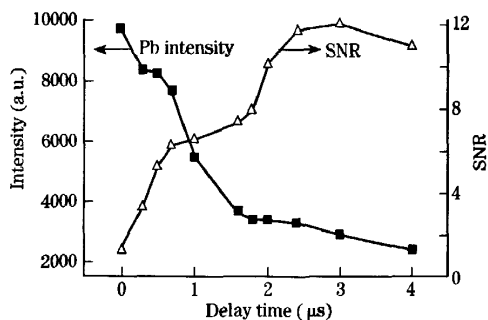


Fig. 2. Intensity and SNR at various delay time.

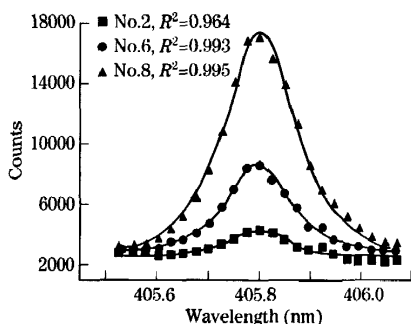


Fig. 3. Fitting curves of 405.78-nm line profiles.

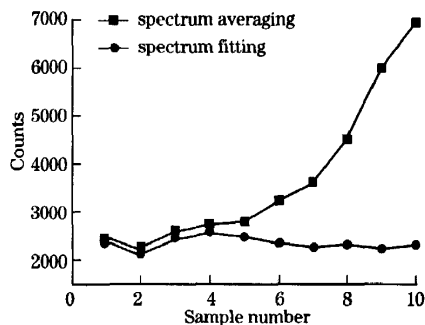


Fig. 4. Spectral background obtained by different methods.

counted by this way is generally affected by the profile broadening of the analyzed spectral line and the other adjacent high-intensity spectral line. In this work, the fitting curve of the spectral line profile is proposed to confirm the spectral background. The line broadening mechanism of LIBS mainly includes Doppler broadening which results in a Gaussian line profile, natural broadening, and collision broadening which lead to a symmetric Lorentz profile. Actually, the measuring line profile is the Voigt profile obtained by convolution of the above two profiles<sup>[1]</sup>. But in typical LIBS conditions, the Stark broadening caused by the collision of electrons and ions is the main contribution that dominates the line profile, so the Lorentzian function is used to fit the spectral line.

Figure 3 shows three fitting results of Pb 405.78-nm lines in the LIBS of soil samples with different lead contents, and the data are fitted by a symmetric Lorentzian

distribution. The goodness of fit is satisfying, especially for the higher intensity spectra. According to the fitting curve, the information about the FWHM and the bottom asymptote of the spectral line can be gained. The value of FWHM will be used in the self-absorption correction model, and the value of the horizontal bottom asymptote is considered as the value of background.

The values of spectral background, obtained respectively by the method of curve fitting and from the mean of bottom side spectra of analyzed line, are compared in Fig. 4. The values of background gained from two approaches are almost equivalent when the lead content is low (the intensity of Pb 405.78-nm line is small accordingly). But along with the increase of lead content in samples, the mean of bottom side spectra increases sharply and the value of the horizontal bottom asymptote is standing at an even level. The experimental conditions for all the samples are the same and the matrix component of samples varies slightly, and thus it is reasonable that the background for all the samples keeps in a certain level. The increase of the mean of bottom side spectra beside the analyzed line does not truly reflect the variation of spectral background. In fact, it is impacted by the wide range broadening profile of the high intensity 405.78-nm line as the lead content increasing.

Ten soil samples as shown in Table 1 were put into the experiment, and the average spectrum of 10 laser shots was used for the calibration analysis of every sample. The background intensities of 405.78-nm line were calculated by the fitting curves. The calibration analysis of emission spectroscopy is generally based on the Lomakin-Scherbe equation of<sup>[12]</sup>

$$I = aC^b, \tag{8}$$

where  $I$  is the spectrum intensity of the analysis,  $C$  is the elemental concentration of analysis species,  $a$  is a constant parameter based on the experiment, and  $b$  is the self-absorption parameter varying from 0.5 to 1 according to the self-absorption degree.

Thus, if the self-absorption of analytic line is absent, the calibration curve between  $I$  and  $C$  should be linear. When the self-absorption is considered, the logarithm form ( $\lg I$  versus  $\lg C$ ) is usually used for the linear calibration, and the parameter  $b$  is assumed to be a constant less than 1. Actually, the parameter  $b$  varies along with the change of elemental concentration of analysis species in samples, thus it cannot really remove the self-absorption effect.

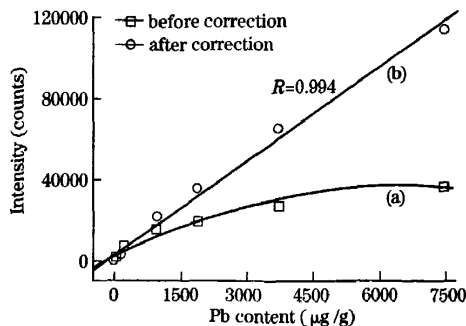


Fig. 5. Calibration curves (a) before and (b) after self-absorption correction.

**Table 2. Comparison of Relative Deviation Before and After Self-Absorption Correction (%)**

| No.    | 1     | 2    | 3    | 4    | 5    | 6    | 7    | 8   | 9   | 10  |
|--------|-------|------|------|------|------|------|------|-----|-----|-----|
| Before | 121.7 | 51.6 | 14.9 | 23.2 | 14.3 | 12.8 | 19.1 | 9.1 | 6.3 | 9.2 |
| After  | 10.3  | 4.9  | 5.7  | 7.3  | 7.9  | 2.4  | 5.1  | 3.7 | 2.7 | 1.3 |

The curve (a) in Fig. 5 presents the relation between the net line intensity of Pb 405.78 nm and the lead concentration. An obvious bending is observed when the lead concentration is high, which is the typical symbolization of self-absorption happening. The occurrence of emission line self-absorption makes the line intensity lower than it should be, and consequently affects the precision of calibration analysis.

A correcting process, aiming at the emission line self-absorption of Pb 405.78 nm, is executed using the introduced correction model. The electron density of plasma is counted by the information of Al 394.40-nm emission line, which is considered as no self-absorption happening because the aluminum concentration is checked at a very low level in these samples. According to the electron density  $n_e$  and the FWHM  $\Delta\lambda$  of spectral line 405.78 nm, the SAC can be solved and used to correct the influence of self-absorption. The line (b) in Fig. 5 is the new calibration curve fitted by the intensity data after correction. It shows that the application of the self-absorption correction changes the line intensity little in the low lead content samples since the weak self-absorption, and improves the line intensity markedly when the lead concentration in the samples increases. And a good linear calibration curve is obtained after self-absorption correction.

Table 2 shows the relative standard deviation of calibration analysis using the original data and the data after correction. The occurrence of line self-absorbing in samples with high lead contents damages badly the calibrating precision and the accuracy of element quantitative analysis, especially for the sample with lower concentration of analytic element, in which the equal absolute error leads to much higher relative analytical error. That is why bigger relative deviation presents in the samples with lower lead content. After the self-absorption correction of the emission line 405.78 nm, the analytical precision is improved obviously. The results show that the correction model is very effective for the improvement of LIBS quantitative analysis when self-absorption occurs.

Also, the self-absorption correction is proved to be helpful for improving the detection limit of lead in soil. The detection limit ( $C_L$ ) for element analysis is calculated from the calibration curve by using<sup>[13]</sup>

$$C_L = 3S_{ave}/m, \quad (9)$$

where  $S_{ave}$  is the average of the standard deviations of the measurements for the samples with five lowest element concentrations, and  $m$  is the slope of the calibration curve. This correcting process not only decreases

the standard deviation of the measurement, but also increases slope of the calibration curve as shown in the Fig. 5. In this work, the detection limit of lead in soil is optimized to 8  $\mu\text{g/g}$ .

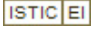
In conclusion, we have designed a typical LIBS experiment for the detection of the lead content in soil. The intensive self-absorption of Pb 405.78-nm line presents in the samples with high lead content and badly damages the calibrating precision of quantitative analysis. A correction model for emission line self-absorption, based on the information of line broadening in the analytical spectrum and the Stark broadening parameter, is introduced and used to calculate the degree of line self-absorption and then correct the line intensity. The results show that this correction model is very effective to improve the LIBS calibrating measurement when the analytical spectral line is obviously self-absorbed in the optically thick plasma. The feasibility and precision of detecting the lead pollution in soil by LIBS are verified.

This work was supported by the National Natural Science Foundation of China (Nos. 50576029 and 50646037) and the Specialized Research Fund for the Doctoral Program of Higher Education (No. 20020487013).

## References

1. D. A. Cremers and L. J. Radziemski, *Handbook of Laser-Induced Breakdown Spectroscopy* (Wiley, Chichester, 2006).
2. A. W. Miziolek, V. Palleschi, and I. Schechter, (eds.) *Laser-Induced Breakdown Spectroscopy (LIBS): Fundamental and Applications* (Cambridge University Press, Cambridge, 2006).
3. C. Pasquini, J. Cortez, L. M. C. Silva, and F. B. Gonzaga, *J. Braz. Chem. Soc.* **18**, 463 (2007).
4. H. Xu, S. Guan, Y. Fu, X. Zhang, X. Xu, X. Ji, E. Feng, R. Zheng, and Z. Cui, *Chinese J. Lasers* (in Chinese) **34**, 577 (2007).
5. R. Shu, H. Qi, G. Lü, D. Ma, Z. He, and Y. Xue, *Chin. Opt. Lett.* **5**, 58 (2007).
6. L. Wang, C. Zhang, and Y. Feng, *Chin. Opt. Lett.* **6**, 5 (2008).
7. C. Aragón, J. Bengoechea, and J. A. Aguilera, *Spectrochim. Acta Part B* **56**, 619 (2001).
8. D. Bulajic, M. Corsi, G. Cristoforetti, S. Legnaioli, V. Palleschi, A. Salvetti, and E. Tognoni, *Spectrochim. Acta Part B* **57**, 339 (2002).
9. V. Lazic, R. Barbini, F. Colao, R. Fantoni, and A. Palucci, *Spectrochim. Acta Part B* **56**, 807 (2001).
10. R. Mavrodineanu and H. Boiteux, *Flame Spectroscopy* (Wiley, New York, 1965).
11. A. M. El Sherbini, Th. M. El Sherbini, H. Hegazy, G. Cristoforetti, S. Legnaioli, V. Palleschi, L. Pardini, A. Salvetti, and E. Tognoni, *Spectrochim. Acta Part B* **60**, 1573 (2005).
12. L. Yu, J. Lu, W. Chen, G. Wu, K. Shen, and W. Feng, *Plasma Sci. Technol.* **7**, 3041 (2005).
13. F. J. Wallis, B. L. Chadwich, and R. J. S. Morrison, *Appl. Spectrosc.* **54**, 1231 (2000).

# Correction and analysis of lead content in soil by laser-induced breakdown spectroscopy

作者: [Chengli Xie](#), [Jidong Lu](#), [Pengyan Li](#), [Jie Li](#), [Zhaoxiang Lin](#)  
作者单位: [Chengli Xie, Jidong Lu, Pengyan Li, Jie Li \(State Key Laboratory of Coal Combustion, Huazhong University of Science and Technology, Wuhan 430074, China\)](#), [Zhaoxiang Lin \(College of Electrics and Information Engineering, South-Central University for Nationalities, Wuhan 430074, China\)](#)  
刊名: [中国光学快报 \(英文版\)](#)   
英文刊名: [CHINESE OPTICS OF LETTERS](#)  
年, 卷(期): 2009, 7(6)  
被引用次数: 0次

## 参考文献(13条)

1. [D A Cremers](#), [L J Radziemski](#) [Handbook of Laser-Induced Breakdown Spectroscopy](#) 2006
2. [A W Miziolek](#), [V Palleschi](#), [I Schechter](#) [Laser-Induced Breakdown Spectroscopy \(LIBS\): Fundamental and Applications](#) 2006
3. [C Pasquini](#), [J Cortez](#), [L M C Silva](#), [F B Gonzaga](#) [查看详情](#) 2007
4. [H Xu](#), [S Guan](#), [Y Fu](#), [X Zhang](#), [X Xu](#), [X Ji](#), [E Feng](#), [R Zheng](#), and [Z Cui](#) [查看详情](#) 2007
5. [R Shu](#), [H Qi](#), [G Lii](#), [D Ma](#), [Z He](#) and [Y Xue](#) [查看详情](#) 2007
6. [L Wang](#), [C Zhang](#), [Y Feng](#) [查看详情](#) 2008
7. [C Aragon](#), [J Bengoechea](#), [J A Aguilera](#) [查看详情](#) 2001
8. [D Bulajic](#), [M Corsi](#), [G Cristoforetti](#), [S Legnaioli](#), [V Palleschi](#), [A Salvetti](#) and [E Tognoni](#) [查看详情](#) 2002
9. [V Lazic](#), [R Barbini](#), [F Colao](#), [R Fantoni](#) and [A Palucci](#) [查看详情](#) 2001
10. [R Mavrodineanu](#), [H Boiteux](#) [Flame Spectroscopy](#) 1965
11. [A M El Sherbini](#), [Th M El Sherbini](#), [H Hegazy](#), [G Cristoforetti](#), [S Legnaioli](#), [V Palleschi](#), [L Pardini](#), [A Salvetti](#) and [E Tognoni](#) [查看详情](#) 2005
12. [L Yu](#), [J Lu](#), [W Chen](#), [G Wu](#), [K Shen](#) and [W Feng](#) [查看详情](#) 2005
13. [F J Wallis](#), [B L Chadwich](#), [R J S Morrison](#) [查看详情](#) 2000

本文链接: [http://d.wanfangdata.com.cn/Periodical\\_zgjg-e200906029.aspx](http://d.wanfangdata.com.cn/Periodical_zgjg-e200906029.aspx)

授权使用: 河北工业大学图书馆(wfhbgydx), 授权号: 6fd76234-56ec-452e-866a-9ecd01672111

下载时间: 2011年4月22日